

# The Local Group as an Astrophysical Laboratory for Massive Star Feedback

By M. S. OEY<sup>1</sup>

<sup>1</sup>Lowell Observatory, 1400 W. Mars Hill Rd., Flagstaff, AZ 86001, USA

The feedback effects of massive stars on their galactic and intergalactic environments can dominate evolutionary processes in galaxies and affect cosmic structure in the Universe. Only the Local Group offers the spatial resolution to quantitatively study feedback processes on a variety of scales. Lyman continuum radiation from hot, luminous stars ionizes H II regions and is believed to dominate production of the warm component of the interstellar medium (ISM). Some of this radiation apparently escapes from galaxies into the intergalactic environment. Supernovae and strong stellar winds generate shell structures such as supernova remnants, stellar wind bubbles, and superbubbles around OB associations. Hot ( $10^6$  K) gas is generated within these shells, and is believed to be the origin of the hot component of the ISM. Superbubble activity thus is likely to dominate the ISM structure, kinematics, and phase balance in star-forming galaxies. Galactic superwinds in starburst galaxies enable the escape of mass, ionizing radiation, and heavy elements. Although many important issues remain to be resolved, there is little doubt that feedback processes plays a fundamental role in energy cycles on scales ranging from individual stars to cosmic structure. This contribution reviews studies of radiative and mechanical feedback in the Local Group.

---

## 1. Introduction

The Local Group is especially suited as a laboratory for studying the effects of the massive star population on the galactic environment. There are three types of massive star feedback: 1. Radiative feedback, i.e., ionizing emission, which results in photoionized nebulae and diffuse, warm ( $10^4$  K) ionized gas; 2. Mechanical feedback, predominantly from supernovae (SNe), resulting in supernova remnants (SNRs), superbubbles, and galactic superwinds; and 3. Chemical feedback from nucleosynthesis in SNe and massive star evolution, which drives galactic chemical evolution. Since the last will be reviewed by Don Garnett and Monica Tosi in this volume, I will address here only the radiative and mechanical feedback processes.

Only in the Local Group can we spatially resolve the the various physical parameters that determine, and result from, the interaction of massive stars with their immediate environment. Radiative and mechanical feedback return large quantities of energy to the galactic environment, both with luminosities  $\log L$  of order  $36 - 41 \text{ erg s}^{-1}$  for typical OB associations. These processes may dominate the balance between different temperature phases of the interstellar medium (ISM), profoundly affecting the structure and kinematics of the ISM, star formation, and other evolutionary processes in star-forming galaxies.

## 2. Radiative Feedback

Photoionization results in H II regions and ionized gas, which are especially familiar and photogenic in the Milky Way and Magellanic Clouds.

### 2.1. *Nebular emission-line diagnostics*

The nebular emission-line spectra offer vital diagnostics of conditions in these regions, and are especially powerful if modeled with tailored photoionization models. However, a

class of “semi-empirical” line diagnostics are widely used to probe nebular parameters. For example, the parameter (Vílchez & Pagel 1988)

$$\eta' \equiv \frac{[\text{O II}]\lambda 3727 / [\text{O III}]\lambda\lambda 4959, 5007}{[\text{S II}]\lambda 6724 / [\text{S III}]\lambda\lambda 9069, 9532} \quad (2.1)$$

and  $[\text{Ne III}]/\text{H}\beta$  (Oey et al. 2000) probe the ionizing stellar effective temperature, while the parameters (Pagel et al. 1979)

$$R23 \equiv ([\text{O II}]\lambda 3727 + [\text{O III}]\lambda\lambda 4959, 5007) / \text{H}\beta \quad (2.2)$$

and (Vílchez & Esteban 1996; Christensen et al. 1997)

$$S23 \equiv ([\text{S II}]\lambda 6724 + [\text{S III}]\lambda\lambda 9069, 9532) / \text{H}\beta \quad (2.3)$$

estimate the oxygen and sulfur abundances. Using observations of LMC H II regions, Oey & Shields (2000) question the reliability of  $S23$  and show that

$$S234 \equiv ([\text{S II}]\lambda 6724 + [\text{S III}]\lambda\lambda 9069, 9532 + [\text{S IV}]10.5\mu) / \text{H}\beta \quad , \quad (2.4)$$

a superior diagnostic of sulfur abundance, can be easily estimated from optical line strengths. All of these semi-empirical diagnostics must first be similarly tested and calibrated using objects with independently constrained parameters. The Local Group offers by far the best nebular samples in which to simultaneously: obtain spectral classifications of the ionizing stars; evaluate the gas morphology relative to the ionizing stars, thereby constraining the nebular ionization parameter; and estimate the abundances. These are the three primary parameters that determine the nebular emission. Thus, having empirical constraints on photoionization models, the behavior of the emission-line diagnostics can be calibrated. The nebular emission can also be used to constrain the hot stellar atmosphere models themselves, since these NLTE, expanding atmospheres are complicated and difficult to model. Such studies have been carried out for O and WR stars in the Magellanic Clouds and the Galaxy (Oey et al. 2000; Kennicutt et al. 2000; Crowther et al. 1999).

Another important test is to evaluate the degree to which H II regions are indeed radiation-bounded, as is normally assumed; the escape of ionizing radiation is a critical question for the ionization of the diffuse, warm ionized medium (see below), as well as the use of H recombination emission as a star formation tracer. The escape of ionizing radiation from the host galaxies themselves is also vital to understanding the ionization state of the intergalactic medium (IGM) and the reionization of the early Universe. We can test whether H II regions are radiation-bounded by simply comparing the observed stellar spectral types, and thus inferred ionizing flux, with the observed nebular emission. Currently, it appears that while most nebulae are radiation-bounded, a large subset apparently are density-bounded (Oey & Kennicutt 1997; Hunter & Massey 1990).

With adequate calibrations of nebular diagnostics against Local Group objects, we can infer various physical parameters for distant, unresolved star-forming regions.

## 2.2. *Statistical properties of H II regions*

Statistical properties of H II region populations offer important quantitative characterizations of global star formation in galaxies. The H II region luminosity function (H II LF) reveals the relative importance of major star-forming events, hosting super star clusters, and smaller, ordinary OB associations. The H II LF has been determined for many nearby galaxies, including all of the star-forming galaxies in the Local Group (Milky Way: Smith & Kennicutt 1989, McKee & Williams 1997; Magellanic Clouds, M31, M33: Kennicutt et al. 1989, Walterbos & Braun 1992, Hodge et al. 1999; IC 10, Leo A, Sex A, Sex B, GR8,

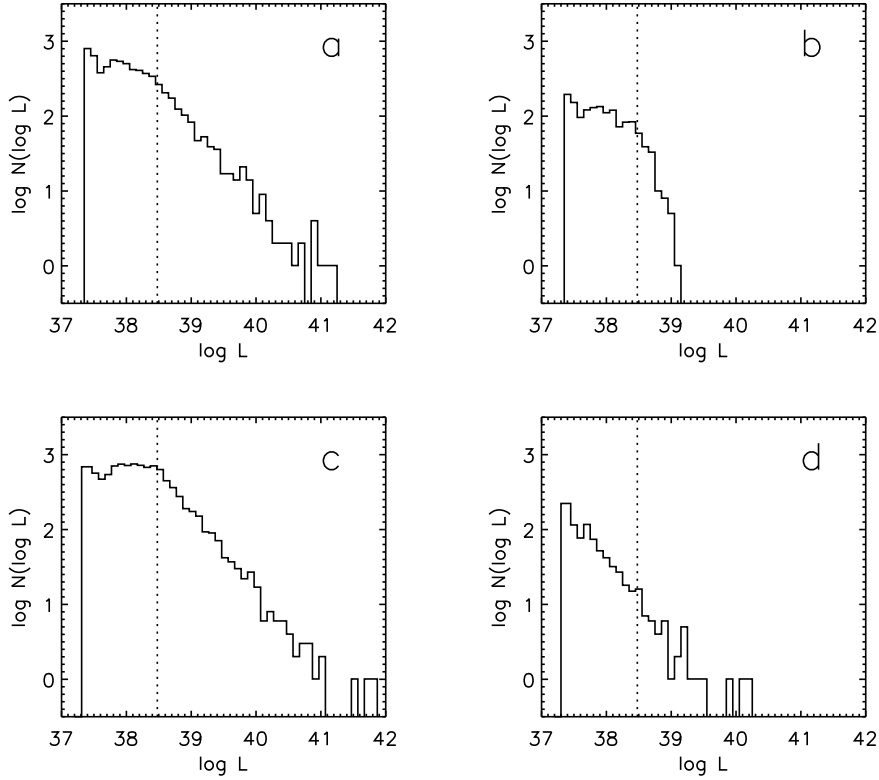


FIGURE 1. Monte Carlo models of the H II LF from Oey & Clarke (1998a): (a) constant nebular creation rate for a full power law in  $N_*$  given by equation 2.6; (b) continuous creation with an upper cutoff in  $N_*$  of 10 ionizing stars; (c) zero-age instantaneous burst for all objects, with a full power law in  $N_*$ ; (d) the evolved burst in (c) after 7 Myr. The maximum stellar ionizing luminosity in the IMF here corresponds to  $\log \mathcal{L} = 38.5$  (vertical dotted line).

Peg, WLM; Youngblood & Hunter 1999). There is agreement that the H II LF universally appears to be described by a power law:

$$N(\mathcal{L}) d\mathcal{L} \propto \mathcal{L}^{-a} d\mathcal{L} \quad , \quad (2.5)$$

with a power-law index  $a \sim 2$  for the differential LF. Figure 1 presents Monte Carlo models by Oey & Clarke (1998a) that show the existence of a flatter slope below  $\log \mathcal{L} \sim 37.5 - 38.5$ , owing to a transition at low luminosity to objects dominated by small number statistics in the ionizing stellar population. We also see that the H II LF can offer some insights on the nature and history of the very most recent global star formation, within the last  $\sim 10$  Myr.

The observed behavior of the H II LF is consistent with the existence of a universal power law for the number of ionizing stars  $N_*$  per cluster (Oey & Clarke 1998a):

$$N(N_*) dN_* \propto N_*^{-2} dN_* \quad . \quad (2.6)$$

This is consistent with direct observations of the cluster luminosity and mass functions in a variety of regimes (see Chandar, this volume; Elmegreen & Efremov 1997; Meurer et al. 1995; Harris & Pudritz 1994). Such a universal power-law for the cluster mass function is

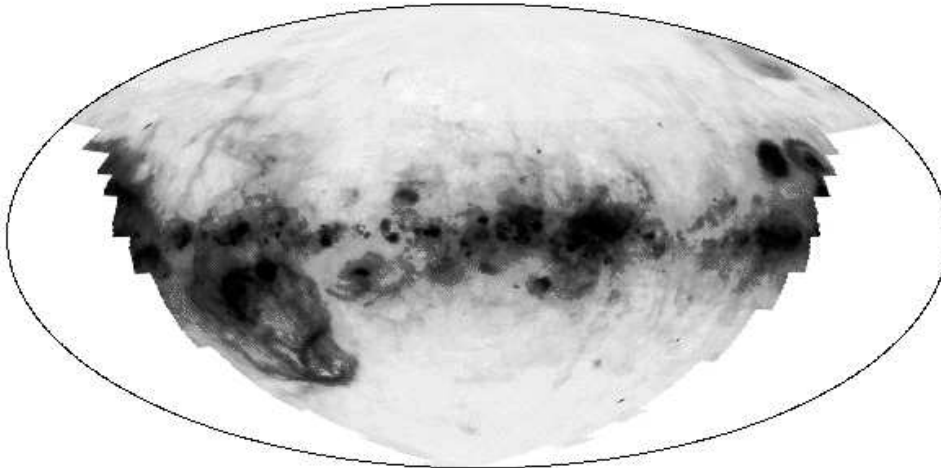


FIGURE 2. WHAM H $\alpha$  survey of the Milky Way warm ionized medium, centered at  $l = 120^\circ$  (Reynolds 1998; <http://www.astro.wisc.edu/wham/>).

fundamental, similar to the stellar initial mass function (IMF; e.g., Oey & Muñoz-Tuñón 2003).

The nebular size distribution has also been determined in many galaxies, although it has been studied in less detail than the H II LF (Milky Way, Magellanic Clouds, M31, M33, NGC 6822: van den Bergh 1981, Hodge et al. 1999; IC 10, Leo A, Sex A, Sex B, GR8, Peg, WLM: Hodge 1983, Youngblood & Hunter 1999). In his pioneering work, van den Bergh (1981) described the size distribution as an exponential:

$$N_R \propto e^{-R/R_0} \quad . \quad (2.7)$$

However, this relation is difficult to reconcile with the power-law form of the H II LF. To first order, the H $\alpha$  luminosity  $\mathcal{L}$  should scale with the volume emission as  $R^3$ , and thus the size distribution should have a similar power-law form to that of the H II LF, but with exponent  $b = 2 - 3a$ . We can see in Figure 1a and c that the existence of the turnover in the H II LF described above can cause the entire H II LF to mimic an exponential form. Thus we suggest that the intrinsic form of the size distribution is also a power-law relation:

$$N(R) dR \propto R^{-b} dR \quad . \quad (2.8)$$

With a slope also flattening below a value of  $\log R \sim 130$  pc, corresponding to the transition in the H II LF above, this form of the size distribution is also a good description of the available data (Oey et al. 2003). Our initial investigation shows good agreement between observations and the predicted value for  $b = 4$ , implied by the H II LF slope  $a = 2$ .

### 2.3. Warm Ionized Medium

Another global effect of radiative feedback is the diffuse, warm ionized medium (WIM). This  $10^4$  K component of the ISM contributes  $\sim 40\%$  of the total H $\alpha$  luminosity in star-forming galaxies for a wide variety of Hubble types (e.g., Walterbos 1998). In the Galaxy, the WIM has a scale height of  $\sim 1$  kpc, temperature of  $\sim 8000$  K, and mean density  $\sim 0.025$  cm $^{-3}$  (Minter & Balsaer 1997). While it has long been thought that massive stars dominate its ionization (e.g., Frail et al. 1991; Reynolds & Tufté 1995), contributions from other processes also appear to be necessary. Dissipation of turbulence

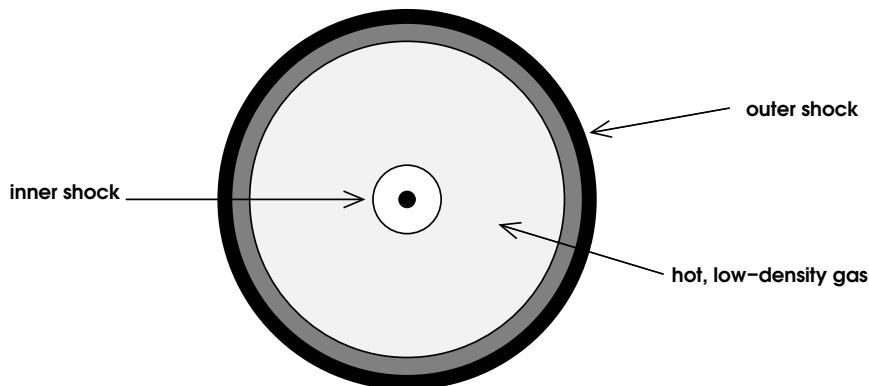


FIGURE 3. The adiabatic wind-driven bubble model (see text). The shell at the outer shock consists of swept-up ISM on the outside and shocked wind material on the inside, separated by a contact discontinuity.

(Minter & Spangler 1997; Minter & Balser 1997) and photoelectric heating (Reynolds & Cox 1992) are among the suggested heating candidates in our Galaxy.

The WIM is most often studied through optical nebular emission. For the Galaxy, the largest optical survey is from the Wisconsin  $H\alpha$  Mapper (WHAM) project (Reynolds et al. 1998; Figure 2). In addition to  $H\alpha$ , the WHAM Fabry-Perot data also include observations of [S II] $\lambda 6717$ , [N II] $\lambda\lambda 6583, 5755$ , [O III] $\lambda 5007$ , He I  $\lambda 5876$ , and other nebular emission lines. The other disk galaxies in the Local Group have also been studied optically: the LMC (Kennicutt et al. 1995), M31 (Galarza et al. 2000; Greenawalt et al. 1997; Walterbos & Braun 1992, 1994), M33 (Hoopes & Walterbos 2000), and NGC 55 (Otte & Dettmar 1999; Ferguson et al. 1996).

Other techniques, notably at radio wavelengths, are available for studying the WIM in the Milky Way. These offer additional probes of the WIM distribution and filling factor. Heiles et al. (1998) observed radio recombination lines in the Galaxy, and Frail et al. (1991) examined lines of sight through the WIM via pulsar dispersion measures. Faraday rotation obtained through radio polarimetry has been exploited by e.g., Uyaniker et al. (2003), Gray et al. (1999), and Minter & Spangler (1996); this technique is also used by Berkhuijsen et al. (2003) for M31.

### 3. Mechanical Feedback

Supernova (SN) explosions of massive stars are a dominant source of kinetic energy in the interstellar medium. Strong, supersonic stellar winds are also an important source in the case of the extreme most massive stars ( $\gtrsim 40M_{\odot}$ ). Mechanical feedback structures the ISM, with immediate consequences corresponding to supernova remnants (SNRs), stellar wind-driven bubbles, and superbubbles resulting from combined SNe and winds from multiple stars.

While the SNRs evolve, in the simplest description, according to the Sedov (1959) model, the wind-driven bubbles and superbubbles are thought to evolve according to a similar, Sedov-like adiabatic model for constant energy input (Pikel’ner 1968; Castor et al. 1977): the central supersonic wind drives a shock into the ambient ISM, piling up a radiatively cooled, dense shell; and a reverse shock near the source thermalizes the wind’s kinetic energy, thereby generating a hot ( $10^6 - 10^7$  K), low-density ( $n \sim 10^{-2} - 10^{-3} \text{ cm}^{-3}$ ) medium that dominates the bubble volume (Figure 3). This heating process is believed to be the origin of the diffuse hot, ionized medium (HIM) in the

interstellar medium. Assuming that the hot bubble interior remains adiabatic, the self-similar shell evolution follows the simple analytic relations,

$$\begin{aligned} R &\propto (L/n)^{1/5} t^{3/5} \quad , \\ v &\propto (L/n)^{1/5} t^{-2/5} \quad , \end{aligned} \quad (3.1)$$

where  $R$  and  $v$  are the shell radius and expansion velocity,  $L$  is the input mechanical power, and  $t$  is the age. Once SNe begin to explode, they quickly dominate  $L$ , and the standard treatment is to consider the discrete SNe as a constant energy input (e.g., Mac Low & McCray 1988). Hence, we may write  $L$  in terms of the SN parameters:

$$L = N_* E_{51} / t_e \quad , \quad (3.2)$$

where  $N_*$  is the number of SNe,  $E_{51}$  is the SN energy, and  $t_e$  is the total time during which the SNe occur.

There are several approaches to testing the standard, adiabatic shell evolution, and by extension, our understanding of mechanical feedback. In the first instance, we can examine the properties and kinematics of individual shell systems and carry out rigorous comparisons with the model predictions. Secondly, we can also examine statistical properties of entire shell populations in galaxies, and compare with model predictions. And thirdly, we can carry out spatial correlations of shells with regions of recent star formation, to confirm the existence of putative stellar progenitors. All three of these methods require high spatial resolution, and thus the Local Group offers by far the best, and often the only feasible, laboratory.

### 3.1. *Individual shell systems*

A number of individual superbubbles exhibit multi-phase ISM, as is qualitatively predicted by the adiabatic shell model. DEM L152 (N44) in the Large Magellanic Cloud (LMC) is a beautiful example where the nebular ( $10^4$  K) gas in the shell clearly confines the hot, X-ray-emitting ( $10^6$  K) gas within (Magnier et al. 1996; Figure 4). Chu et al. (1994) also confirmed the existence of C IV and Si IV absorption in the lines of sight toward all stars within LMC superbubbles. These tracers of intermediate temperature ( $10^5$  K) gas are expected in interface regions between hot and cold gas. Quantitatively, however, the detected X-ray emission from LMC superbubbles has been an order of magnitude higher than predicted by the adiabatic model. It is therefore thought that the anomalous emission results from impacts to the shell wall by internal SNRs (Chu & Mac Low 1990; Wang & Helfand 1991), a scenario which is supported by other signatures such as enhanced [S II]/H $\alpha$  and anomalous kinematics (Oey 1996; see below). Many other superbubbles have not been detected in X-rays, although the upper limits tend to be high, and remain within the model predictions. It is hoped that the capabilities of *Chandra* and *XMM* will be applied to these objects.

Since most early-type stars are found in OB associations, wind-driven bubbles of individual massive stars are rare, and consequently few quantitative studies of these objects exist. In principle, O stars offer the most straightforward test of the standard shell evolution, since their wind histories are simple and relatively well-understood. One of the few such studies was carried out by Oey & Massey (1994) on two nebular bubbles around individual late-type O stars in M33. They found crude consistency with the model predictions, but the constraints are limited by lack of kinematic information. Cappa and collaborators (e.g., Cappa & Benaglia 1999; Benaglia & Cappa 1999; Cappa & Herbstmeier 2000) have studied a number of H I shells around Of stars, which are presumably evolved O stars. They generally find a significant growth-rate discrepancy such that the shells appear to be too small for the assumed stellar wind power. Wolf-Rayet (W-R)

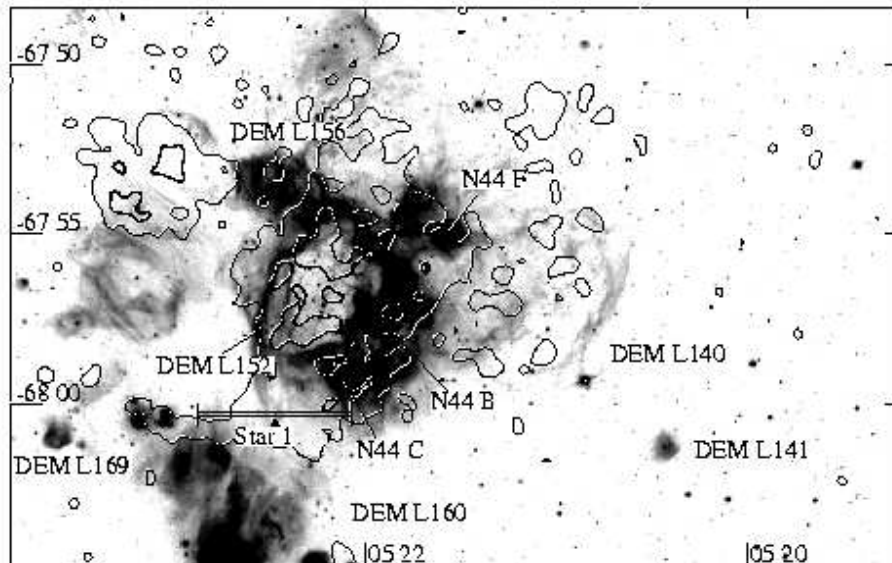


FIGURE 4.  $H\alpha$  image of superbubble DEM L152 (N44) in the LMC, with *ROSAT* X-ray contours overlaid (from Magnier et al. 1996).

stars are well-known to have the most powerful stellar winds, and a number of W-R ring nebulae have also been examined kinematically. Optical studies include those by Treffers & Chu (1982), García-Segura & Mac Low (1995), and Drissen et al. (1995); while, e.g., Arnal et al. (1999) and Cappa et al. (2002) examine the neutral and radio continuum properties. The W-R nebulae are also apparently too small, but owing to the complicated stellar wind history and associated environment, it is more difficult to interpret the W-R shell dynamics.

Superbubbles around OB associations are much larger, brighter, and easier to identify than single star wind-driven bubbles, and consequently have been much more actively studied. They are especially prominent in the LMC, where the proximity and high galactic latitude offer a clear, detailed view of the objects. The most comprehensive study of superbubble dynamics was carried out by Oey and collaborators (Oey 1996; Oey & Smedley 1998; Oey & Massey 1995) on a total of eight LMC objects. Saken et al. (1992) and Brown et al. (1995) also examined two Galactic objects. All of these are young, nebular superbubbles having ages  $\lesssim 5$  Myr. These studies again consistently reveal a growth-rate discrepancy equivalent to an overestimate in the inferred  $L/n$  by up to an order of magnitude. About half of the objects also show anomalously high expansion velocities, implying a strong, rapid shell acceleration from the standard evolution.

A number of factors could be individually, or collectively, responsible for these dynamical discrepancies. The first possibility is a systematic overestimate in  $L/n$ : stellar wind parameters remain uncertain within factors of 2 – 3. The ambient density distribution is also critical to the shell evolution; as shown by Oey & Smedley (1998), a sudden drop in density can cause a “mini-blowout” of the shell, whose kinematics can reproduce those of the high-velocity LMC shells. In the case of those objects, however, the presence of anomalously high X-ray emission favors the SNR impact hypothesis discussed above. In any case, the critical role of the ambient environment motivated us to map the HI distribution around three superbubbles in the LMC sample (Oey et al. 2002). The results were surprisingly inhomogeneous, with one object essentially in a void, another with sig-

nificant H I in close proximity, and a third with no correspondence at all between the nebular and neutral gas. Thus it is virtually impossible to infer the ambient H I properties for any given object without direct observations. This heterogeneity suggests that a systematic underestimate of  $n$  is not responsible for the universal growth-rate discrepancy. However, a related environmental parameter is the ambient pressure. If the ISM pressure has been systematically underestimated, then the superbubble growth would become pressure-confined at an earlier, smaller stage. We are currently exploring this possibility (Oey & García-Segura 2003, in preparation).

Finally, if the superbubble interiors are somehow cooling, then the shells will no longer grow adiabatically. While this possibility has been explored theoretically from several angles, there is as yet no empirical evidence, in particular, radiation, that the objects are cooling. Meanwhile, mass-loading has long been a candidate cooling mechanism (e.g., Cowie et al. 1981; Hartquist et al. 1986), either by evaporating material from the shell wall, or by ablating clumps that are overrun by the shell. The enhanced density would then increase the cooling rate of the hot interior. More recently, Silich et al. (2001) and Silich & Oey (2002) suggested that the metallicity increase expected from the parent SN explosions can significantly enhance the cooling and X-ray emission, especially for extremely low metallicity systems.

### 3.2. *Global Mechanical Feedback*

Another approach to understanding superbubble evolution is in examining the statistical properties of superbubble populations in galaxies. It is possible to derive the distributions in, for example, size and expansion velocity from equations 3.1 and assumptions for the mechanical luminosity function (MLF), object creation rate, and ambient parameters. Oey & Clarke (1997) analytically derived the superbubble size distribution for simple combinations of creation rate and MLF. They found that the size distribution is dominated by pressure-confined objects that are no longer growing, following a differential distribution in radius  $R$ :

$$N(R) dR \propto R^{1-2\beta} dR \quad , \quad (3.3)$$

where  $\beta$  is the power-law slope of the MLF  $\phi(L)$  for the form,  $\phi(L) \propto L^{-\beta}$ . Since the mechanical power  $L$  is determined by the SN progenitors (equation 3.2), the MLF to first order has the universal power-law slope of  $-2$  given by equation 2.6. Equation 3.3 shows that the form of the MLF turns out to be a vital parameter in determining the size distribution. For the MLF slope  $\beta = 2$ , the size distribution  $N(R) dR \propto R^{-3} dR$ . There is a peak in  $N(R)$ , corresponding to the stall radius of the lowest- $L$  objects, which would be individual SNRs in this analysis (Figure 5).

This prediction can be compared to the observed size distribution of H I shells that have been catalogued in the largest Local Group galaxies. By far the most complete catalog is that for the Small Magellanic Cloud (SMC; Staveley-Smith et al. 1997). The companion survey for the LMC (Kim et al. 1999) surprisingly shows about four times *fewer* shells than the SMC, in spite of the former's much larger size. The number of H I shells in the LMC is also much smaller than expected from the number of H II regions, whereas their relative numbers are fully consistent with their respective life expectancies in the SMC (Oey & Clarke 1997). Thus it appears that some process may be destroying the LMC shells prematurely, perhaps merging, shearing in the disk, or other ISM dynamical processes related to the high LMC star-formation rate and/or disk morphology. In contrast, the SMC has a more 3-dimensional, solid-body kinematic structure, and thus offers a better ISM for comparison with the crude size distribution predictions.



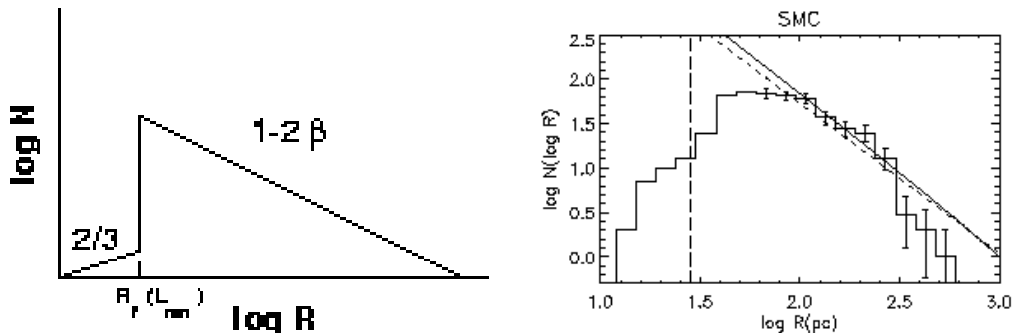


FIGURE 5. *Left*: Schematic representation of the predicted superbubble size distribution for a power-law MLF of slope  $-\beta$  and constant object creation rate. *Right*: Comparison of slope (dotted line) fitted to the observed size distribution of H I shells in the SMC and predicted slope (solid line; from Oey & Clarke 1997).

For the SMC, the observed H I shell size distribution has a slope of  $-2.7 \pm 0.6$ , in remarkable agreement with the predicted slope of  $-2.8 \pm 0.4$  derived from the actual H II LF (Oey & Clarke 1997; Figure 5). This suggests that the bubbly structure in the neutral ISM of this galaxy can be entirely attributed to mechanical feedback. It is also worth noting that a size distribution of fractal holes can be derived from the same dataset (Stanimirović et al. 1999). The power-law slope of  $-3.5$  for the holes is similar, but different, from that for the shells, so it will be extremely interesting to make further such comparisons in other galaxies.

H I shell catalogs also have been compiled for M31 (Brinks & Bajaja 1986) and M33 (Deul & den Hartog 1990). These older catalogs lack sensitivity and resolution, but preliminary comparisons of the shell size distributions are broadly in agreement with the prediction (Oey & Clarke 1997). A modern H I survey of M33 by Thilker et al. (2000) is also eagerly anticipated. For the Milky Way, no complete samples of H I shells exist, but the International Galactic Plane Surveys (IGPS; e.g., McClure-Griffiths et al. 2002) may eventually yield data useful for a statistically significant sample.

Similarly, it is possible to derive the distribution in expansion velocities for the shells. Oey & Clarke (1998b) find,

$$N(v) dv \propto v^{-7/2} dv \quad , \quad \beta > 3/2 \quad . \quad (3.4)$$

Again, comparison with the SMC catalog shows consistency with the prediction, although with much larger uncertainty in the observed slope of  $-2.9 \pm 1.4$ . Although taken from the same dataset, this comparison examines a different subset of objects, since the shells with non-negligible expansion velocities clearly sample the growing objects, whereas the size distribution is dominated by pressure-confined, stalled objects.

The Local Group galaxies, especially the Magellanic Clouds, also provide an opportunity to examine the detailed morphology of the ISM. An especially compelling discussion is presented by Elmegreen et al. (2001), who compare the structural morphology of the neutral ISM in the LMC with a fractal model. They show that the LMC's ISM is clearly more filamentary than accounted for in their simple fractal model (Figure 6). Such filamentary structure can be attributed at least in part to the superbubble structuring caused by mechanical feedback. Oey (2002) reviews H I structure in the ISM and argues that the origin of filamentary structure is key to understanding the dynamical and evolutionary processes in the ISM, such as phase balance and star formation.

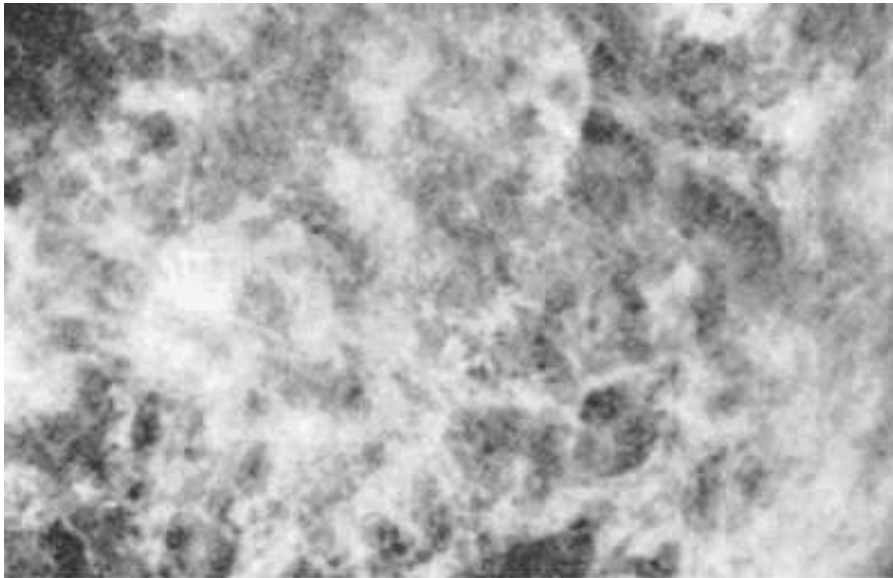


FIGURE 6. H I distribution in a central region of the LMC (white is positive), showing a filamentary ISM morphology that is inconsistent with simple fractal models (from Elmegreen et al. 2001).

### 3.3. Correspondence with Star Formation

Modern studies that compare the spatial distribution of H I shells and star-forming regions show perhaps surprisingly ambiguous results. The galaxy that has been most actively studied in this respect recently is Holmberg II. At a distance of 3 Mpc, Ho II is not a member of the Local Group, and the conflicting results in the literature may be symptomatic of the difficulty with spatial resolution at that distance. While Rhode et al. (1999) failed to identify H I shell progenitor populations from *BVR* aperture photometry, Stewart et al. (2000) did find a positive spatial correlation with star-forming regions using FUV data from the *Ultraviolet Imaging Telescope (UIT)* and  $H\alpha$  observations. Tongue & Westpfahl (1995) also found that the SN rate implied by the radio continuum emission is consistent with the total, integrated superbubble energy in Ho II.

The Magellanic Clouds, and other nearby Local Group galaxies, are clearly superior candidates for investigating quantitative spatial correlations. Kim et al. (1999) have carried out a preliminary study that compares the H I shell properties with those of the OB associations and nebular emission. They are able to identify an evolutionary sequence such that the shells with associated  $H\alpha$  emission show higher expansion velocities than those showing only the presence of OB stars, and the latter in turn show higher  $v$  than the remainder of the shells. The  $H\alpha$  emission also shows smaller radial extent, remaining within that of the H I shells. These trends are consistent with an age sequence and feedback origin for the neutral shells. We are currently carrying out a more detailed follow-up of this study using *UIT* and new optical data (Oey et al. 2003, in preparation).

### 3.4. Interstellar Porosity

A conventional parameterization for global mechanical feedback in galaxies is the interstellar porosity, or volume filling factor of superbubbles. Having derived analytic expressions for the superbubble size distribution, it is straightforward to derive expressions for the porosity (Oey & Clarke 1997). This can be written in terms of the star formation

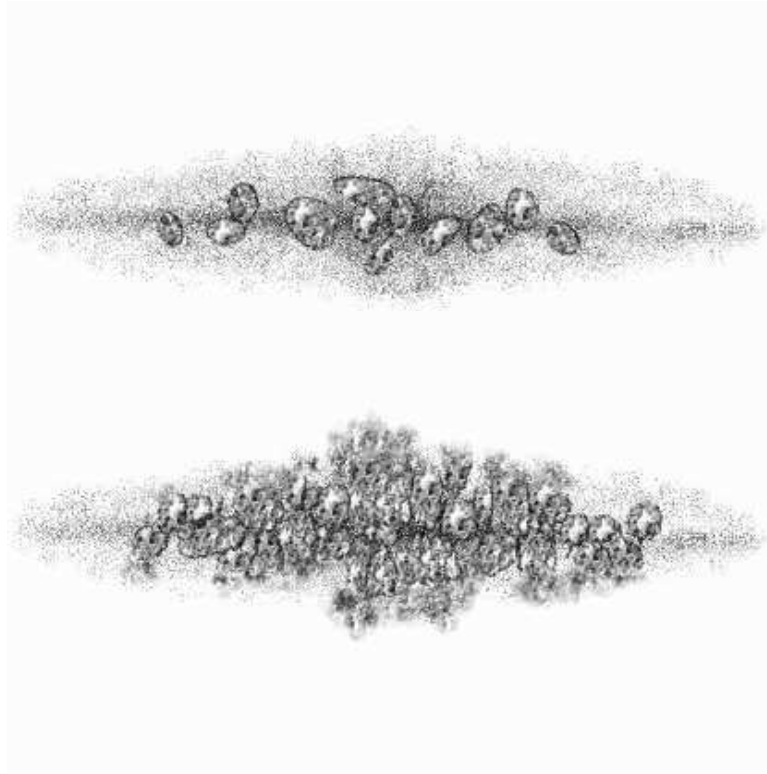


FIGURE 7. Low and high interstellar porosities are shown schematically in the upper and lower panels, respectively. The lower panel shows how  $Q = 1$  defines a threshold porosity and star-formation rate for galactic outflows and escape of ionizing radiation.

rate (SFR), galactic scale height  $h$ , and galactic star-forming radius  $R_g$  (Oey et al. 2001):

$$Q \simeq 16 \frac{\text{SFR}(\text{M}_\odot \text{ yr}^{-1})}{h R_g^2 (\text{kpc}^3)} \quad , \quad (3.5)$$

for Milky Way ISM parameters and Salpeter (1955) IMF. The porosity also can be written in terms of galactic parameters, i.e., ISM mass and velocity dispersion (Clarke & Oey 2002). Assuming a feedback origin for the HIM, the interstellar porosity quantifies the relative phase balance between the HIM and cooler ISM phases.  $Q$  greater than a critical value of unity therefore indicates an outflow condition for the hot gas, as might be encountered in a starburst situation (Figure 7).

For the Local Group star-forming galaxies, Oey et al. (2001) find  $Q \ll 1$  in almost all cases, suggesting that the HIM generally does not dominate the ISM volume. The LMC, however, does show  $Q \sim 1$ . The Milky Way situation is ambiguous, with different estimates of the SFR yielding  $Q$  in the range 0.2 to 1. The truly glaring exception is the starburst galaxy IC 10, for which  $Q \gtrsim 20$ , clearly fulfilling the outflow or superwind criterion. Clarke & Oey (2002) also posit the critical  $Q = 1$  condition as a threshold for radiative feedback to the IGM. Once mechanical outflow is established, the merging and blowout of superbubbles also opens free pathways for ionizing photons to escape from the parent galaxy. They apply this simple model to a variety of phenomena, ranging from giant molecular clouds to Lyman break galaxies.

#### 4. Conclusion

It is clear that both radiative and mechanical feedback energies can dominate evolutionary processes in star-forming galaxies, although we still lack understanding of important aspects in the feedback processes. The extreme range in scale over which feedback has influence is especially remarkable. In addition, it is also possible to investigate and parameterize chemical feedback with analogous methods (e.g., Oey 2000, 2003).

Radiative feedback is responsible for the nebular emission-line diagnostics and tracers of star formation, as well as the WIM component of the ISM. On a detailed level, the line diagnostics still need improved calibrations and photoionization modeling to increase their utility and parameter space. The H II LF is emerging as a quantitative diagnostic of global star formation in galaxies, and reveals a universal law in the stellar membership function for massive stars (equation 2.6). The ionization and energy budget of the WIM, while apparently tied to massive stars, remains to be better understood. Ultimately, the escape of ionizing radiation beyond the parent galaxies bears upon the intergalactic environment and reionization of the early Universe.

Mechanical feedback indisputably drives shell structures that are ubiquitous in the ISM: SNRs, stellar wind-driven bubbles, and superbubbles. The standard, adiabatic model for the evolution of the bubbles and superbubbles is broadly consistent with a variety of empirical evidence; yet, quantitatively, a number of outstanding problems remain. The late evolution of the shells is especially enigmatic and critical for understanding the role of feedback in generating the HIM, as well as the global properties of the ISM. Spatial correlations of interstellar shells with star-forming regions still need to firmly establish the physical processes and interactions related to feedback. Preliminary studies of the size and velocity distributions of H I shells appear to confirm a dominant role for mechanical feedback in structuring the ISM. This analytic analysis can be extended to parameterize the interstellar porosity, implying a critical threshold for the outflow of superwinds, heavy elements, and ionizing radiation.

I am grateful to the conference organizers and STScI for supporting in part this contribution to the Symposium.

#### REFERENCES

- Arnal, E. M., Cappa, C. E., Rizzo, J. R., Cichowolski, S. 1999, *AJ*, 118, 1798  
 Berkhuisen, E. M., Beck, R., & Hoernes, P. 2003, *A&A*, 398, 937  
 Benaglia, P. & Cappa, C. E. 1999, *A&A*, 346, 979  
 Brinks E., Bajaja E. 1986, *A&A*, 169, 14  
 Brown, A. G. A., Hartmann, D., & Burton, W. B. 1995, *A&A*, 300, 903  
 Cappa, C. E. & Benaglia, P. 1998, *AJ*, 116, 1906  
 Cappa, C. E., Goss, W. M., & Pineault, S. 2002, *AJ*, 123, 3348  
 Cappa, C. E. & Herbstmeier, U. 2000, *AJ*, 120, 1963  
 Castor, J., McCray, R., & Weaver, R. 1975, *ApJ*, 200, L107  
 Christensen, T., Petersen, L., & Gammelgaard, P., 1997, *AA*, 322, 41  
 Cowie, L. L., McKee, C. F., & Ostriker, J. P. 1981, *ApJ*, 247, 908  
 Chu, Y.-H. & Mac Low, M.-M., 1990, *ApJ*, 365, 510  
 Chu, Y.-H., Wakker, B., Mac Low, M.-M., & García-Segura, G. 1994, *AJ*, 108, 1696  
 Clarke, C. J. & Oey, M. S. 2002, *MNRAS*, 337, 1299  
 Crowther, P. A., Pasquali, A., De Marco, O., Schmutz, W., Hillier, D. J., & de Koter, A., 1999, *A&A*, 350, 1007  
 Deul E. R., den Hartog R. H. 1990, *A&A*, 229, 362  
 Drissen, L., Moffat, A. F. J., Walborn, N. R., & Shara, M. R. 1995, *AJ*, 110, 2235

- Elmegreen, B. G. & Efremov, Y. N. 1997, ApJ, 480, 235
- Elmegreen, B. G., Kim, S., & Staveley-Smith 2001, ApJ, 548, 749
- Ferguson, A. M. N., Wyse, R. F. G., & Gallagher, J. S. 1996, AJ, 112, 2567
- Frail, D. A., Cordes, D. M., Hankins, T. H., & Weisberg, J. M. 1991, ApJ, 382, 168
- Galarza, V. C., Walterbos, R. A. M., & Braun, R. 1999, AJ, 118, 2775
- García-Segura, G. & Mac Low, M.-M. 1995, ApJ, 455, 145
- Gray, A. D., Landecker, T. L., Dewdney, P. E., Taylor, A. R., Willis, A. G., & Normandeau, M. 1999, ApJ, 514, 221
- Greenawalt, B., Walterbos, R. A. M., & Braun, R. 1997, ApJ, 483, 666
- Hartquist, T. W., Dyson, J. E., Pettini, M., & Smith, L. J. 1986, MNRAS, 221, 715
- Harris, W. E. & Pudritz, R. E. 1994, ApJ, 429, 177
- Heiles, C., Koo, B.-C., Levenson, N. J. A., & Reach, W. T. 1996, ApJ, 462, 326
- Hodge, P. W., Balsley, J., Wyder, T. K., & Skelton, B. P. 1999, PASP, 111, 685
- Hoopes, C. G. & Walterbos, R. A. M. 2000, ApJ, 541, 597
- Hunter, D. A. & Massey, P. 1990, AJ, 99, 846
- Kennicutt, R. C., Bresolin, F., Bomans, D. J., Bothun, G. D., & Thompson, I. B. 1995, AJ, 109, 594
- Kennicutt, R. C., Bresolin, F., French, H., & Martin, P. 2000, ApJ, 537, 589
- Kennicutt, R. C., Edgar, B. K., & Hodge, P. W. 1989, ApJ, 337, 761
- Kim, S., Dopita, M. A., Staveley-Smith, L., & Bessell, M. S. 1999, AJ, 118, 2797
- Mac Low, M.-M. & McCray, R. 1988, ApJ, 324, 776
- Magnier, E. A., Chu, Y.-H., Points, S. D., Hwang, U., & Smith, R. C. 1996, ApJ, 464, 829
- McClure-Griffiths, N. M., Dickey, J. M., Gaensler, B. M., & Green, A. J. 2002, ApJ, 578, 176
- McKee C. F. & Williams J. P. 1997, ApJ, 476, 144
- Meurer, G. R., Heckman, T. M., Leitherer, C., Kinney, A., Robert, C., & Garnett, D. R. 1995, AJ, 110, 2665
- Minter, A. H. & Balseer, D. S. 1997, ApJ, 484, L133
- Minter, A. H. & Spangler, S. R. 1996, ApJ, 458, 194
- Minter, A. H. & Spangler, S. R. 1997, ApJ, 485, 182
- Oey, M. S. 1996, ApJ, 467, 666
- Oey, M. S., 2000, ApJ, 542, L25
- Oey, M. S., 2002, in *Seeing Through the Dust: The Detection of H I and the Exploration of the ISM in Galaxies*, eds. R. Taylor, T. Landecker, & A. Willis, (San Francisco: ASP), 295
- Oey, M. S., 2003, MNRAS, 339, 849
- Oey, M. S. & Clarke, C. J. 1997, MNRAS, 289, 570
- Oey, M. S. & Clarke, C. J. 1998a, AJ, 115, 1543
- Oey, M. S. & Clarke, C. J. 1998b, in *Interstellar Turbulence*, eds. J. Franco & A. Carramiñana, Cambridge: Cambridge Univ. Press, 112
- Oey, M. S., Clarke, C. J., & Massey, P. 2001, in *Dwarf Galaxies and their Environment*, eds. K. de Boer, R.-J. Dettmar, & U. Klein, (Shaker Verlag), 181
- Oey, M. S., Dopita, M. A., Shields, J. C., & Smith, R. C. 2000, ApJS, 128, 511
- Oey, M. S., Groves, B., Staveley-Smith, L., & Smith, R. C. 2002, AJ, 123, 255
- Oey, M. S. & Kennicutt, R. C., MNRAS, 291, 827
- Oey, M. S. & Massey, P., 1994, ApJ, 425, 635
- Oey, M. S. & Massey, P., 1995, ApJ, 452, 210
- Oey, M. S. & Muñoz-Tuñón, C. 2003, in *Star Formation Through Time*, eds. E. Pérez, R. González-Delgado, & G. Tenorio-Tagle, (San Francisco: ASP), in press
- Oey, M. S., Parker, J. S., Mikles, V. J., & Zhang, X. 2003, AJ, submitted
- Oey, M. S. & Shields, J. C. 2000, ApJ, 539, 687
- Oey, M. S. & Smedley, S. A. 1998, AJ, 116, 1263
- Otte, B. & Dettmar, R.-J. 1999, A&A, 343, 705
- Pagel, B. E. J., Edmunds, M. G., Blackwell, D. E., Chun, M. S., & Smith, G., 1979, MNRAS, 189, 95
- Pikel'ner S. B. 1968, Astrophys. Lett. 2, 97
- Reynolds, R. J. & Cox, D. P. 1992, ApJ, 400, L33

- Reynolds, R. J. & Tufte, S. L. 1995, ApJ, 439, L17
- Reynolds, R. J., Tufte, S. L., Haffner, L. M., Jaehnig, K., & Percival, J. W., 1998, PASA, 15, 14
- Rhode, K. L., Salzer, J. J., Westpfahl, D. J., & Radice, L. A. 1999, AJ, 118, 323
- Saken, J. M., Shull, J. M., Garmany, C. D., Nichols-Bohlin, J., & Fesen, R. A. 1992, ApJ, 397, 537
- Salpeter, E. E. 1955, ApJ, 121, 161
- Sedov, L. I. 1959, *Similarity and Dimensional Methods in Mechanics*, Academic, New York.
- Silich, S. A., Tenorio-Tagle, G., Terlevich, R., Terlevich, E., & Netzer, H. 2001, MNRAS, 324, 191
- Silich, S. A. & Oey, M. S. 2002, in *Extragalactic Star Clusters*, IAU Symposium 207, eds. D. Geisler, E. K. Grebel, & D. Minniti, (San Francisco: ASP), 459
- Smith T. R. & Kennicutt R. C. 1989, PASP, 101, 649
- Stanimirović, S., Staveley-Smith, L., Dickey, J. M., Sault, R. J., & Snowden, S. L. 1999, MNRAS, 302, 417
- Staveley-Smith, L., Sault, R. J., Hatzidimitriou, D., Kesteven, M. J., & McConnell, D. 1997, MNRAS 289, 225
- Stewart, S. G., *et al.* 2000, ApJ, 529, 201
- Thilker, D. A., Braun, R., & Walterbos, R. A. M. 2000, BAAS, 197, #38.08
- Tongue, T. D. & Westpfahl, D. J. 1995, AJ, 109, 2462
- Treffers, R. R. & Chu, Y.-H. 1982, ApJ, 254, 569
- Uyaniker, B., Landecker, T. L., Gray, A. D., & Kothes, R. 2003, ApJ, 585, 785
- van den Bergh, S., 1981, AJ, 86, 1464
- Vílchez, J. M. & Esteban, C. 1996, MNRAS, 290, 265
- Vílchez, J. M. & Pagel, B. E. J., 1988, MNRAS, 231, 257
- Walterbos, R. A. M. 1998, PASA, 15, 99
- Walterbos, R. A. M. & Braun, R. 1992, A&AS, 92, 625
- Walterbos, R. A. M. & Braun, R. 1992, ApJ, 431, 156
- Wang, Q. & Helfand, D. J. 1991, ApJ, 373, 497
- Youngblood, A. J. & Hunter, D. A. 1999, ApJ, 519, 55